Post-disaster Recovery of Hybrid AC/DC Cyber-physical Distribution Systems with Adaptive Switching of VSC Control Modes and Scheduling of Multi-type Repair Resources

Xuyuan Gong, Kaigui Xie, Changzheng Shao, Yifan Su, Bo Hu, and Dong Zheng

***Abstract*—The form of hybrid AC/DC is a trend in power distribution systems. The resilience against extreme weather depends on the coordination of cyber and physical systems. Therefore, it is necessary to study the post-disaster recovery of AC/DC hybrid cyber-physical distribution systems (CPDSs). Voltage source converters (VSCs) are critical cyber-physical devices in hybrid AC/DC distribution systems (HDSs) that offer flexibility in post-disaster recovery. However, existing literature on the role of VSC commonly ignores the unreliable communication. In this paper, we quantify the impact of communication failures on VSCs and propose an adaptive switching model of VSC control modes that enhances both the emergency islanding and service restoration phases of post-disaster recovery. This paper also introduces a scheduling model of multi-type repair resources including power failure repair crews, communication failure repair crews, and emergency communication vehicles for joint the restoration of CPDSs. The system recovery model is also presented. Finally, a novel optimization framework combining adaptive switching of VSC control modes, scheduling of multi-type repair resources, and system recovery is proposed to improve the post-disaster recovery efficiency. The effectiveness and superiority of the proposed framework are demonstrated through numerical experiments in a modified IEEE 123-bus system.**

***Index Terms*—Hybrid AC/DC distribution system, cyber-physical distribution system, resilience, repair resource, voltage source converter, post-disaster recovery.**

NOMENCLATURE

A. Sets and Indices

Ω_{VSC}, Ω_{RCS}	Sets of voltage source converters (VSCs) and remote-controlled switches (RCSs)
γ	Index of repair resources *pfrc*, *cfrc*, and *ecv*
a, b	Indices for vertices V_{ecv}^{CN}
B_{VSC}	Set of lines where VSC is located
c, C	Index and set for cyber blind areas
DP	Set of depots
$dp(\gamma)$	Index for depot where repair resource γ departs and returns
dp	Index for depot
$ds(i)$, $us(i)$	Sets of downstream and upstream nodes connected to node i
$e(c)$	Index for vertex V_{cfrc}^{CN} resulting in cyber blind area c
i, j	Indices for electric and communication nodes
ij	Index for lines
k	Index for VSC in Ω_{VSC} or RCS in Ω_{RCS}
ka, kd	Indices for nodes on AC and DC sides of VSC
m, n	Indices for vertices V_{pfrc}^{EN}
N_c	Set of nodes in cyber blind area c
N, B	Sets of electric or communication nodes and lines
N^{AC}, B^{AC}	Sets of electric or communication nodes and lines in AC grid
N^{DC}, B^{DC}	Sets of electric or communication nodes and lines in DC grid
N_{VSC}^{AC}, N_{VSC}^{DC}	Sets of nodes on AC and DC sides of VSC
N_G	Sets of nodes configured with distributed generator (DG)
N_a, B_a	Sets of nodes and links in communication node block a
N_{sub}	Set of substation nodes
NB_a	Set of nodes and links in block a
$O(\gamma)$	Index for starting vertices of repair resource γ
p, q	Indices for vertices V_{cfrc}^{CN}
pfrc, *cfrc*, *ecv*	Indices for power failure repair crew (PFRC), communication failure repair crew (CFRC), and emergency communication vehicle (ECV)

Manuscript received: February 19, 2025; revised: June 25, 2025; accepted: August 20, 2025. Date of CrossCheck: August 20, 2025. Date of online publication: September 5, 2025.

This work was supported by the National Key Research and Development Program of China (No. 2023YFA1011304).

X. Gong, K. Xie (corresponding author), C. Shao, Y. Su, B. Hu, and D. Zheng are with the National Key Laboratory of Power Transmission Equipment Technology, Chongqing University, Chongqing 400044, China (e-mail: 1223551365@qq.com; kaiguixie@vip.163.com; cshao@cqu.edu.cn; hboy8361@163. com; suyf@cqu.edu.cn; 565638589@qq.com).

DOI: 10.35833/MPCE.2025.000145

t, τ Indices for time period

T^{p} Set of time period

$T(\gamma)$ Index for ending vertices of repair resource γ

V_{pfrc}^{EN}, V_{cfrc}^{CN} Sets of depots and electric or communication failures in system graph

V_{ecv}^{CN} Set of depots, RCSs, and VSCs in power system

B. Parameters

ω_i Priority of load at node i

D Number of depots

$l_{dp,m}$ Path distance from fault at vertex m to depot dp

M, ζ A large number and a small number for modeling and linearization

P_i^{load}, Q_i^{load} Active and reactive load demands at electric node i

$P_i^{\mathrm{G,max}}$, $Q_i^{\mathrm{G,max}}$ The maximum generation limits of active and reactive power at electric node i

$P_{i,j}^{\max}$, $Q_{i,j}^{\max}$ The maximum limits of active and reactive power of electric line ij

$Q_k^{\max}$, $Q_k^{\min}$ The maximum and minimum generation limits of reactive power of VSC k

$R_{i,j}$, $X_{i,j}$ Resistance and reactance of electric line ij

R_k, X_k AC line resistance and reactance

$T_{m,pfrc}^{\mathrm{rep}}$ Time required for *pfrc* to repair power faults at vertex m

$T_{p,cfrc}^{\mathrm{rep}}$ Time required for *cfrc* to repair communication faults at vertex p

T_{ecv}^{op} Operation time after *ecv* arrives in workplace

T_a^{op} Time to operate component a

$T_{m,n,\gamma}^{\mathrm{tra}}$ Travel time for repair resource γ from vertex m to n

$U_i^{\max}$, $U_i^{\min}$ The maximum and minimum voltage limits of electric node i

U_0 Value of reference voltage

$U_{i,t}^{\mathrm{sqr}}$ Squared voltage value at node i during period t

C. Decision Variables

$\alpha_{i,t}$ Energized state of node i during period t

$\alpha_{m,t}^{\mathrm{ER}}$, $\alpha_{a,t}^{\mathrm{CR}}$ Binary variables indicating whether repair of electric or communication failures at vertices m and a is completed during period t

$\beta_{m,t}^{\mathrm{ER}}$, $\beta_{a,t}^{\mathrm{CR}}$ Binary variables indicating whether electric or communication states at vertices m and a are intact during period t

A_i^{CR} Time when communication function of node i is restored

$A_a^{\mathrm{CR,CFRC}}$, $A_a^{\mathrm{CR,ECV}}$ Time when communication function of vertex a is restored by CFRC and ECV

A_a^{CR} Time when communication function of vertex a is restored

$A_{m,pfrc}^{\mathrm{reach}}$, $A_{p,cfrc}^{\mathrm{reach}}$ Time when *pfrc* and *cfrc* reach electric or communication failures or depot at vertices m and p

$A_{a,ecv}^{\mathrm{reach}}$ Time when *ecv* reaches component or depot at vertex a

$A_{T(\gamma)}^{\mathrm{leave}}$ Time when repair resource γ leaves vertice $T(\gamma)$

$A_{m,pfrc}^{\mathrm{leave}}$, $A_{p,cfrc}^{\mathrm{leave}}$ Time when *pfrc* and *cfrc* leave electric or communication failures or depot at vertices m and p

$A_{a,ecv}^{\mathrm{leave}}$ Time when *ecv* leaves component or depot at vertex a

$f_{ij,t}^{\mathrm{AC}}$, $f_{ij,t}^{\mathrm{DC}}$ Binary variables indicating whether node i is the parent of node j during period t

$P_{i,j,t}$, $Q_{i,j,t}$ Active and reactive power of electric line ij during period t

$P_{i,t}$, $Q_{i,t}$ Active and reactive power at node i during period t

$P_{i,t}^{\mathrm{G}}$, $Q_{i,t}^{\mathrm{G}}$ Active and reactive power generated by node i during period t

$P_{k,t}^{\mathrm{VSC}}$, $Q_{k,t}^{\mathrm{VSC}}$ Active and reactive outputs of VSC k during period t

$r_{i,t}$ Binary variable indicating whether node i is root node during period t

$s_{ij,t}^{\mathrm{AC}}$, $s_{ij,t}^{\mathrm{DC}}$ Binary variables indicating energization state of electric line ij in AC and DC grids during period t

$s_{i,t}$ Binary variable indicating energization state of node i during period t

$s_{ij,t}$ Binary variable indicating energization state of electric line ij during period t

$T_{a,ecv}^{\mathrm{stay}}$ Time that *ecv* stays at vertex a

$U_{i,t}$ Voltage of node i during period t

$U_{i,t}^{\mathrm{VSC}}$ Voltage of VSC at node i during period t

u_a^{ECV}, u_a^{CFRC} Binary variables indicating whether communication function of vertex a is restored by ECV and CFRC

$u_{dp,m}^{\mathrm{FPM}}$, $u_{dp,e}^{\mathrm{FPM}}$ Binary variables indicating whether electric or communication failure at vertices m and e is pre-assignment to depot dp

$x_{m,n,pfrc}$ Binary variable indicating whether a *pfrc* travels from vertex m to n

$x_{p,q,cfrc}$ Binary variable indicating whether a *cfrc* travels from vertex p to q

$x_{a,b,ecv}$ Binary variable indicating whether an *ecv* travels from vertex a to b

$x_{dp(\gamma),T(\gamma),\gamma}$ Binary variable indicating whether a repair resource γ travels from vertex $dp(\gamma)$ to $T(\gamma)$

z_c^{comp} Binary variable indicating whether all communication failures leading to cyber blind area c have been repaired

$y_{ij,t}^{\mathrm{AC}}$ Connection state of line ij during period t

I. Introduction

THE rapidly increasing integration of renewable energy and power electronic loads accelerates the development of AC/DC hybrid distribution systems (HDSs) [1], [2]. The

coordination between AC and DC distribution systems is heavily reliant on communication and control technologies. It is necessary to regard HDSs as cyber-physical distribution systems (CPDSs) considering the coupling between cyber and physical systems. Given the increasing deployment of smart inverters, distributed energy resource management systems, and advanced communication protocols in modern distribution systems, the CPDS is not merely a future-oriented concept, but has become a realistic representation of operation context nowadays. Especially, under contingencies, the coupling between cyber and physical systems significantly hinders the recovery process and impairs the system efficiency in quickly restoring the load [3]. For instance, in 2024, typhoon Capricorn caused severe damage to the CPDSs in southern China. The inefficiency in service restoration was exacerbated by large-scale communication disruptions [4]. Therefore, it is crucial to improve the post-disaster recovery capability of HDSs under the coupling between cyber and physical systems.

Voltage source converters (VSCs) are significant cyber-physical coupled devices in HDSs [5]. They integrate AC and DC distribution systems by enabling bidirectional AC/DC conversion based on operation requirements. From the perspective of distribution system restoration (DSR), VSCs can provide critical flexibility in two phases, i.e., emergency power supply and service restoration [6]. In the first phase, the VSC control mode can be adjusted following fault isolation to provide voltage support for the islanded system, thereby ensuring uninterrupted power supply in non-faulted areas [7], [8]. In the second phase, the VSC control mode can be quickly switched according to the repair process, and then its continuous power control capability can be utilized to restore more loads, thus improving the efficiency of service restoration [9], [10].

However, existing studies commonly overlook the effect of reliable communication infrastructures in exploiting the flexibility of VSCs in DSR [11], [12]. Communication failures or delays may disrupt the execution of the VSC control and its effect on power control [13]. Therefore, it is impractical to utilize the VSC in DSR without considering the communication impacts, yet this issue has been largely overlooked in prior studies. Consequently, there is an urgent need for HDS recovery that simultaneously restores cyber and physical systems via multiple repair resources. Concretely, we consider the coupling between cyber and physical systems and quantify the impact of communication failures on VSCs. In this situation, the exploitation of VSC flexibility in DSR requires further investigation. Meanwhile, the widely used scheduling model that only considers power repair resources will no longer be applicable, inspiring us to exploit the characteristics of different resources for repairing power and communication failures. Moreover, in the context of coupling between cyber and physical systems, a novel optimization framework is needed to enhance the efficiency of DSR through the simultaneous optimization of the adaptive switching of VSC control modes, the scheduling of multi-type repair resources, and the system recovery.

Fully controlled VSCs provide continuous power control, voltage support, and rapid switching of control modes. In the emergency power supply phase, the system is islanded with voltage support from the VSC, thus ensuring uninterrupted power supply to non-faulted areas. In the service restoration phase, VSCs offer greater flexibility during system topology changes by switching control modes, which facilitates the coordination with repair resources and accelerates the DSR process. Therefore, an increasing number of studies are considering the use of VSCs to enhance the DSR efficiency.

Some studies have utilized VSC flexibility for emergency power supply. For example, [7] and [8] utilize VSC flexibility for smart islanding partition. However, they either set all VSCs to voltage support mode or set each VSC mode empirically. None of them chose the best control strategy for the current failure situation. In addition to the emergency power supply phase, some studies have investigated the utilization of VSC flexibility in the service restoration phase. In [9], a VSC control mode table is formulated, in which, based on the initial failure situation faced by each VSC, the corresponding control modes can be determined. The system will remain under this control strategy to accomplish the subsequent recovery. Reference [10] considers three possible operation situations that the VSC may face and presets the corresponding control modes. The switching of control modes is performed based on the operation conditions it faces during the recovery process, realizing a certain degree of adaptive switching and greatly improving the exploitation of its flexibility. However, despite these studies involving repair processes and topology changes during the service restoration, the VSC control modes are either kept fixed or empirically adjusted based on the preset operation conditions. There is no adaptive switching tailored to repair and recovery scenarios, resulting in non-optimal control strategy for facilitating the service restoration.

VSCs are cyber-physical coupled devices for the coordination between AC and DC distribution systems that requires robust communication functionalities to fully exploit the flexibility of HDSs during DSR. Similar to the remote control switch (RCS), the control center communicates with the VSC via the communication link to transmit control commands and adjust corresponding variables. Some studies have considered the coupling between cyber and physical systems in traditional AC distribution systems; however, few studies address it in HDSs, which needs advanced communication and control technologies. Therefore, it is essential to consider the CPDSs to explore the underlying mechanisms and quantify the consequences of communication failures on the VSC.

In DSR research, traditional studies have focused solely on power system restoration, emphasizing emergency resource dispatch and system reconfiguration to ensure the power supply. Distributed generators (DGs) [14], [15], energy storage systems [15], [16], and mobile emergency generators [14] have been employed for restoration. As disasters grow more severe, permanent load recovery necessitates the repair of failure, prompting studies to co-optimize the scheduling of repair resources with DSR. Reference [15] proposes

an integrated optimization model coordinating DGs, energy storage systems, reconfiguration, and the scheduling strategy of repair crews and mobile emergency generators to maximize load restoration. References [17] and [18] model the behavioral logic of different repair crews for collaborative DSR.

Recent studies have explored CPDS restoration in AC distribution systems. Reference [19] introduces a spatio-temporal incidence matrix to represent cyber-physical failure correlations. Communication recovery resources such as communication failure repair crews (CFRCs) have also been considered. References [20] and [21] propose collaborative models to schedule repair crews to efficiently repair faults in two systems. Emergency communication resources such as emergency communication vehicles (ECVs) and unmanned aerial vehicles (UAVs) have been deployed to restore control links. Reference [22] employs ECVs to restore communication and control between the control center and the controllable device. Reference [3] integrates UAV into wireless communication for feeder automation. However, few studies address simultaneous restoration of communication and power systems in highly coupled HDSs or the coordination of permanent and emergency communication recovery resources.

The adaptive switching of VSC control modes increases the topology flexibility, and profoundly influences the scheduling of resources and restoration sequencing. Under the coupling between cyber and physical systems, this interaction complicates decision-making even more, rendering prior frameworks insufficient. Therefore, there is an urgent need for a novel optimization framework to simultaneously optimize adaptive switching of VSC control modes, scheduling of multi-type repair resources, and system recovery by capturing the coupling relationships among models.

Overall, the DSR problem of hybrid AC/DC CPDSs has the following challenges: ① how to exploit the capabilities of VSCs to activate the operation flexibility of HDSs across both phases of DSR, thereby enhancing the recovery efficiency; ② how to quantify the impact of communications failures on VSCs, and coordinate multi-type repair resources to jointly repair both power and communication failures; ③ in the context of coupling between cyber and physical systems, a new optimization framework is required to enhance DSR efficiency by simultaneously optimizing the adaptive switching of VSC control modes, the scheduling of multi-type repair resources, and the system recovery.

The main contributions of this paper are threefold.

1) We exploit the capabilities of VSCs to achieve optimal islanding in the emergency power supply phase and adaptive switching of VSC control modes in the service restoration phase. We also leverage the flexibility of HDSs to enhance the recovery efficiency by exploiting the capabilities of VSCs throughout the entire DSR process, from emergency power supply to service restoration.

2) We model the scheduling and operation of three types of repair resources clearly, including both power and communication repair crews. In the CPDSs, we analyze how communication failures impact critical components and quantify their effects. By coordinating two types of communication recovery resources, rather than treating them separately as in traditional methods [21], the restoration efficiency is significantly improved.

3) A novel optimization framework is proposed to jointly optimize the adaptive switching of VSC control modes, the scheduling of multi-type repair resources, and system recovery to further enhance the recovery efficiency.

II. Problem Formulation

As illustrated in Fig. 1, the proposed optimization framework for the DSR of hybrid AC/DC CPDSs consists of several coupled modules. The adaptive switching of VSC control modes, the scheduling of multi-type repair resources, the impact of communications failures, and the system recovery are all considered. In this section, the modeling of the VSC is presented, including operation constraints and switching rules, followed by the scheduling model of multi-type repair resources, the mechanism of communication failures, and the system recovery model. The final optimization framework is developed by coupling these submodels, with the objective function and constraints summarized.

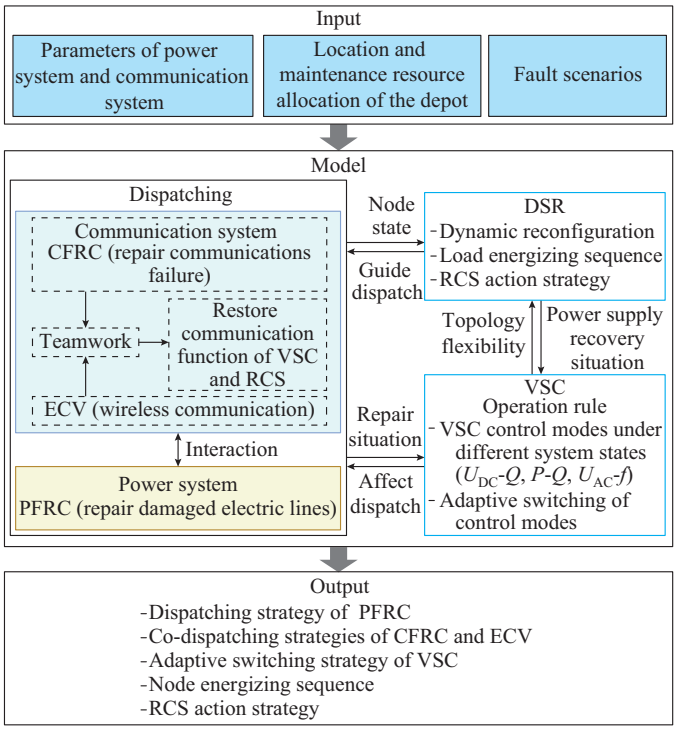

Fig. 1. Proposed optimization framework.

To support the formulation of the optimization framework, several modeling assumptions are introduced to simplify system complexity while preserving essential operation and switching rules.

Assumption 1 (topology consistency assumption): we assume a one-to-one correspondence between power nodes and their associated communication nodes [21], with communication links modeled as wired fiber-optic connections. As a result, the topology of the communication system is consistent with that of the power system [23]. This correspondence describes the observability and controllability to the power

nodes through the communication nodes [21].

Assumption 2 (fault modeling assumption): all physical failures caused by disasters are modeled as binary line states. Binary value of 1 is for operation and 0 is for disconnection, as widely adopted in restoration studies [18], [20]. This assumption effectively captures the impacts of failures and repairs on system components, while also simplifying the repair optimization process for faster and more efficient computation.

A. Modeling of VSC

The HDSs connected via VSCs, as shown in Fig. 2, comprise AC/DC distribution systems, VSC stations, and protection and control equipment.

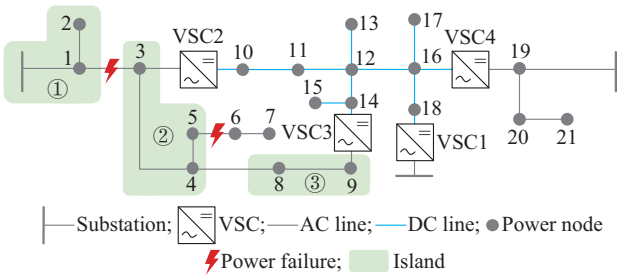

Fig. 2. HDSs connected via VSCs.

The VSCs in the HDSs can be controlled by selecting two variables from active/reactive power and AC/DC voltage, with three main control modes: ① DC voltage and reactive power control (V_{DC}-Q); ② active and reactive power control (P-Q); ③ AC voltage and phase angle control (V_{AC}-f). During normal operation, VSCs in the DC network are coordinated through master-slave control: one VSC acts as the master (V_{DC}-Q) to regulate DC voltage, while others act as slaves (P-Q) to optimize tidal current distribution and balance feeder loads [24].

During faults, the VSC control system collaborates with the distribution automation system for recovery. The fault protection system detects faults, initiates low voltage ride-through (LVRT), locates faults through relays, and controls circuit breakers to isolate faults. Once isolated, the circuit breaker recloses, and the slave VSC switches to V_{DC}-Q or V_{AC}-f control mode to support voltage in non-faulted areas for uninterrupted power supply. At the same time, the main VSC always operates in V_{DC}-Q control mode to regulate the DC grid voltage when the control mode of slave VSC is switched.

It is worth emphasizing that this paper essentially aims to solve an optimization scheduling problem. We simply embed the operation model into the DSR optimization scheduling after switching the VSC control mode. Therefore, detailed control dynamics or implementation methods of the VSC control are not involved in this paper.

1) VSC-oriented System States During Recovery

In HDSs, there are three system states for VSC during the recovery process.

1) Faults occur on both sides of the VSC. The VSC needs to work in the active state; however, due to faults on both sides, it remains inactive.

2) No fault occurs. The master VSC operates in V_{DC}-Q control mode, while the slave VSC operates in P-Q control mode.

3) Fault occurs on one side of the VSC. If the fault occurs on the AC side and the topology reconfiguration process assigns the fault to the corresponding VSC, it switches to the V_{AC}-f control mode. If the fault occurs on the DC side and the topology reconfiguration process assigns the fault to the corresponding VSC, it switches to the V_{DC}-Q control mode.

These corresponding control modes ensures voltage support to non-faulted areas after the LVRT process, enabling uninterrupted power supply. For instance, as illustrated in Fig. 2, VSC2 and VSC3 switch to the V_{AC}-f control mode after fault isolation, with nodes 3 and 9 serving as root nodes of islands ② and ③, respectively, to maintain voltage stability.

However, if the reconfigured topology does not assign a non-faulted area to a specific VSC, that VSC does not need to provide voltage support, regardless of whether the fault is on its AC or DC side, because the non-fault area is already electrically isolated. For example, if the non-fault areas containing nodes 8 and 9 are assigned to VSC2 instead of VSC3, only VSC2 needs to switch to voltage support mode, while VSC3 remains P-Q control mode. Therefore, Fig. 2 merely illustrates the V_{AC}-f control mode of VSC2 and VSC3 and does not necessarily represent the real topology scenarios.

Accurate judgment and adaptive switching of VSC control modes are critical, especially under fault conditions where repair and recovery processes frequently alter the system topology. However, determining the optimal switching strategy remains a challenging and underexplored area.

To systematically define the adaptive switching model, we summarize the system states and corresponding VSC control modes as follows.

1) If a fault is classified on the AC side and the associated AC node lacks a parent node, the VSC switches to the V_{AC}-f control mode.

2) If a fault is classified on the DC side and the associated DC node lacks a parent node, the VSC switches to the V_{DC}-Q control mode.

When a node operates under V_{AC}-f or V_{DC}-Q control mode, its voltage on the faulted side must remain above a predefined threshold to ensure sufficient voltage support, as specified by constraint (1). This constraint guarantees that the root node in islanded operation mode provides adequate voltage magnitude for downstream load restoration. If node i is on the fault side and provides voltage support, we have:

$$U_{i,t}^{\mathrm{VSC}} \geq U_0 \tag{1}$$

It should be noted that the classification of a fault, e.g., whether belonging to the AC or DC side of a VSC, depends on the results of the topology reconfiguration. During the recovery process, the system topology may keep changing. As a result, the classification rules mentioned above are not

fixed and should be interpreted together with the topology reconstruction constraints discussed in the following sections. This introduces a degree of flexibility into the determination process of control mode.

2) Operation Constraints

The equivalent circuit of VSC shown in Fig. 3 includes equivalent impedance and an ideal VSC, connected to AC bus *ka* and DC bus *kd* via circuit breakers. In this paper, it is assumed that these circuit breakers and the connected buses on both sides are included in the VSC station.

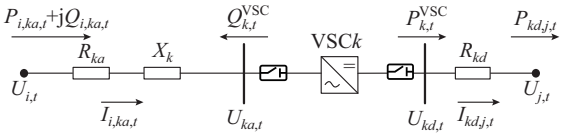

Fig. 3. Equivalent circuit of VSC.

$$\begin{cases} P_{i,ka,t}-I^2_{i,ka,t}R_{ka}=P^{\mathrm{VSC}}_{k,t} \\ P^{\mathrm{VSC}}_{k,t}-I^2_{kd,j,t}R_{kd}=P_{kd,j,t} \\ Q_{i,ka,t}-I^2_{i,ka,t}X_k=-Q^{\mathrm{VSC}}_{k,t} \end{cases} \quad \forall k\in\Omega_{\mathrm{VSC}},\forall t \tag{2}$$

$$\begin{cases} (P^{\mathrm{VSC}}_{k,t})^2+(Q^{\mathrm{VSC}}_{k,t})^2\le(S^{\mathrm{VSC}}_{k})^2 \\ Q^{\min}_{k}\le Q^{\mathrm{vsc}}_{k,t}\le Q^{\max}_{k} \end{cases} \quad \forall k\in\Omega_{\mathrm{VSC}} \tag{3}$$

Constrains (2) and (3) are the power balance constraint and capacity constraint during VSC operation, respectively. Constrains (4) and (5) are the voltage drop balance constraints for the AC/DC lines at both ends of the VSC, respectively.

$$U^2_{i,t}-U^2_{ka,t}=2(R_{i,ka}P_{i,ka,t}+X_{i,ka}Q_{i,ka,t})+(R^2_{i,ka}+X^2_{i,ka})I^2_{i,ka,t} \quad \forall k\in\Omega_{\mathrm{VSC}},\forall t \tag{4}$$

$$U^2_{kd,t}-U^2_{j,t}=2R_{kd,j}P_{kd,t}+R^2_{kd,j}I^2_{kd,j,t} \quad \forall k\in\Omega_{\mathrm{VSC}},\forall t \tag{5}$$

B. Scheduling Model of Multi-type Repair Resources

PFRCs and CFRCs are two types of repairers that repair damaged electrical lines and communication links, respectively. In addition, ECVs can restore the communication functions of VCS and RCS by establishing wireless communication. Their scheduling models are designed to determine the routing and schedule for completing the restoration.

1) Routing Problem

$$\sum_{T(\gamma)}x_{dp(\gamma),T(\gamma),\gamma}=\sum_{O(\gamma)}x_{O(\gamma),dp(\gamma),\gamma}=1 \quad \forall\gamma \tag{6}$$

$$\sum_{T(\gamma)}x_{dp,T(\gamma),\gamma}=\sum_{O(\gamma)}x_{O(\gamma),dp,\gamma}=0 \quad \forall\gamma,\forall dp\in DP\backslash\{dp(\gamma)\} \tag{7}$$

$$\sum_{T(\gamma)}x_{O(\gamma),T(\gamma),\gamma}=\sum_{O(\gamma)}x_{O(\gamma),T(\gamma),\gamma}\le 1 \quad \forall\gamma,\forall k\in V^{MC}\backslash DP \tag{8}$$

Constraints (6) and (7) specify that repair resources γ must return directly to their depot $dp(\gamma)$ without passing through other depots during a task. Constraint (8) ensures continuity in the repair process, requiring that a dispatchable resource γ arrives at a non-depot node, completes its task, and then moves to the next node.

$$\sum_{pfrc}\sum_{m}x_{m,n,pfrc}=1 \quad \forall m\in V^{\mathrm{EN}}_{pfrc},\forall n\in V^{\mathrm{EN}}_{pfrc}\backslash D \tag{9}$$

$$\sum_{cfrc}\sum_{p}x_{p,q,cfrc}\le 1 \quad \forall p\in V^{\mathrm{CN}}_{cfrc},\forall q\in V^{\mathrm{CN}}_{cfrc}\backslash D \tag{10}$$

$$\sum_{ecv}\sum_{a}x_{a,b,ecv}\le 1 \quad \forall a\in V^{\mathrm{CN}}_{ecv},\forall b\in V^{\mathrm{CN}}_{ecv}\backslash D \tag{11}$$

Constraint (9) mandates that each power failure is repaired by one PFRC. Constraints (10) and (11) differ from (9) in two aspects: not all RCSs need to be closed, and CFRCs and ECVs aim to restore communication functions for RCSs and VSCs to ensure controllability when needed. Communication restoration can occur through CFRCs repairing communication links or ECVs providing emergency wireless communication.

2) Scheduling Problem

The scheduling problem is modeled to represent the time relations of the three dispatchable resources in the DSR.

$$\begin{cases} A^{\mathrm{reach}}_{T(\gamma),\gamma}\le A^{\mathrm{reach}}_{O(\gamma),\gamma}+T^{\mathrm{rep}}_{O(\gamma),\gamma}+T^{\mathrm{tra}}_{O(\gamma),T(\gamma),\gamma}+M(1-x_{O(\gamma),T(\gamma),\gamma}) \\ A^{\mathrm{reach}}_{T(\gamma),\gamma}\ge A^{\mathrm{reach}}_{O(\gamma),\gamma}+T^{\mathrm{rep}}_{O(\gamma),\gamma}+T^{\mathrm{tra}}_{O(\gamma),T(\gamma),\gamma}-M(1-x_{O(\gamma),T(\gamma),\gamma}) \end{cases} \quad \forall\gamma\in\{pfrc,cfrc\} \tag{12}$$

$$0\le A^{\mathrm{reach}}_{T(\gamma),\gamma}\le M\sum_{O(\gamma)}x_{O(\gamma),T(\gamma),\gamma} \quad \forall\gamma\in\{pfrc,cfrc\} \tag{13}$$

$$A^{\mathrm{leave}}_{T(\gamma)}=\sum_{\gamma}\left(A^{\mathrm{reach}}_{T(\gamma),\gamma}+T^{\mathrm{rep}}_{T(\gamma),\gamma}\sum_{O(\gamma)}x_{O(\gamma),T(\gamma),\gamma}\right) \quad \forall\gamma\in\{pfrc,cfrc\} \tag{14}$$

For PFRC and CFRC, constraint (12) portrays the time relationship of a resource γ moving between $O(\gamma)$ and $T(\gamma)$ to perform a repair task. Specifically, if γ travels from $O(\gamma)$ to $T(\gamma)$, i. e., $x_{O(\gamma),T(\gamma),\gamma}=1$, γ arrives at $T(\gamma)$ at $A^{\mathrm{reach}}_{T(\gamma),\gamma}=A^{\mathrm{reach}}_{O(\gamma),\gamma}+T^{\mathrm{rep}}_{O(\gamma),\gamma}+T^{\mathrm{tra}}_{O(\gamma),T(\gamma),\gamma}$. If $O(\gamma)$ is a depot, i. e., $O(\gamma)\in DP$, $A^{\mathrm{reach}}_{O(\gamma),\gamma}$ is set to be 0. However, if γ is not dispatched to $T(\gamma)$ to perform the repair work, i.e., $\sum_{O(\gamma)}x_{O(\gamma),T(\gamma),\gamma}=0$, $A^{\mathrm{reach}}_{T(\gamma),\gamma}$ is set to be 0 via constraint (13).

Constraint (14) shows that if γ arrives at $T(\gamma)$ and repairs the corresponding fault, i.e., $\sum_{O(\gamma)}x_{O(\gamma),T(\gamma),\gamma}=1$, it leaves $T(\gamma)$ at $A^{\mathrm{leave}}_{T(\gamma)}=A^{\mathrm{reach}}_{T(\gamma),\gamma}+T^{\mathrm{rep}}_{T(\gamma),\gamma}$. For example, if $\gamma=pfrc$ and $\sum_{m}x_{m,n,pfrc}=1$, the time relationships are given as $A^{\mathrm{reach}}_{n,pfrc}=A^{\mathrm{reach}}_{m,pfrc}+T^{\mathrm{rep}}_{m,pfrc}+T^{\mathrm{tra}}_{m,n,pfrc}$ and $A^{\mathrm{leave}}_{m}=A^{\mathrm{reach}}_{m,pfrc}+T^{\mathrm{rep}}_{m,pfrc}$.

$$\begin{cases} A^{\mathrm{reach}}_{b,ecv}\le A^{\mathrm{reach}}_{a,ecv}+T^{\mathrm{stay}}_{a,ecv}+T^{\mathrm{tra}}_{a,b,ecv}+M(1-x_{a,b,ecv}) \\ A^{\mathrm{reach}}_{b,ecv}\ge A^{\mathrm{reach}}_{a,ecv}+T^{\mathrm{stay}}_{a,ecv}+T^{\mathrm{tra}}_{a,b,ecv}-M(1-x_{a,b,ecv}) \end{cases} \quad \forall a,b\in V^{\mathrm{CN}}_{ecv} \tag{15}$$

$$\begin{cases} 0\le A^{\mathrm{reach}}_{b,ecv}\le M\sum_{a}x_{a,b,ecv} \\ 0\le A^{\mathrm{leave}}_{b,ecv}\le M\sum_{a}x_{a,b,ecv} \end{cases} \quad \forall b\in V^{\mathrm{CN}}_{ecv},\forall ecv \tag{16}$$

$$\begin{cases} A^{\mathrm{leave}}_{b,ecv}\le A^{\mathrm{reach}}_{b,ecv}+T^{\mathrm{stay}}_{b,ecv}+M\left(1-\sum_{a}x_{a,b,ecv}\right) \\ A^{\mathrm{leave}}_{b,ecv}\ge A^{\mathrm{reach}}_{b,ecv}+T^{\mathrm{stay}}_{b,ecv}-M\left(1-\sum_{a}x_{a,b,ecv}\right) \end{cases} \quad \forall b\in V^{\mathrm{CN}}_{ecv} \tag{17}$$

$$\begin{cases} 0\le T^{\mathrm{stay}}_{a,ecv}\le M\sum_{b}x_{b,a,ecv} \\ T^{\mathrm{stay}}_{a,ecv}\ge T^{\mathrm{op}}_{a}+T^{\mathrm{op}}_{ecv}-M\left(1-\sum_{b}x_{b,a,ecv}\right) \end{cases} \quad \forall a\in V^{\mathrm{CN}}_{ecv},\forall ecv \tag{18}$$

For ECV scheduling, constraint (15) indicates that if ECV travels from vertex a to b (i.e., $x_{a,b,ecv}=1$), the ECV arrives at time $A^{\text{reach}}_{b,ecv}=A^{\text{reach}}_{a,ecv}+T^{\text{stay}}_{a,ecv}+T^{\text{tra}}_{a,b,ecv}$. However, if ECV is not dispatched to vertex b, i.e., $\sum_a x_{a,b,ecv}=0$, the arrival time $A^{\text{reach}}_{b,ecv}$ and departure time $A^{\text{leave}}_{b,ecv}$ of vertex b are both 0, as set by constraint (16).

Unlike the PFRC which leaves the vertex immediately after repairing, the ECV requires time to deploy and restore communication at the site, thus ensuring the action of RCS and the switching of VSC. Therefore, constraint (17) ensures that if ECV reaches vertex a, i.e., $\sum_b x_{b,a,ecv}=1$, it waits for the operation to complete before leaving at $A^{\text{leave}}_{b,ecv}=A^{\text{reach}}_{b,ecv}+T^{\text{stay}}_{b,ecv}$. Additionally, $T^{\text{stay}}_{a,ecv}=T^{\text{op}}_{a}+T^{\text{op}}_{ecv}$, as defined by constraint (18).

C. Mechanisms for Impact of Communication Failures

In this paper, the communication system and power distribution system adopt a consistent topology, as described in [23]. Thus, each power node is configured with a corresponding communication node, enabling the control center to observe and control the power components. We group the communication nodes connected to the command center via the same communication feeder into communication node blocks.

When the communication infrastructure is functional, VSCs operate under the coordinated control strategy enabled by high-reliability low-latency communication infrastructure [25]. This allows to synchronize the voltage, frequency, and power flow with other devices in the system, enabling stable AC/DC power exchange. Standard protocols help VSCs respond within sub-second timescales, maintaining system stability and preventing false protection actions [26].

If communication fails, VSCs lose external data and rely only on local measurements. Without system-wide information, control errors may occur, leading to voltage instability, oscillations, or excess current. Uncoordinated responses may also trigger unnecessary protection, causing parts of the system to disconnect and potentially leading to cascading failures [27]. Therefore, reliable communication infrastructure is not merely supportive but foundational to the stable and efficient operation of VSCs.

Therefore, we define cyber blind areas as areas where communication failures prevent nodes from being monitored or controlled. Within these areas, critical devices such as RCSs and VSCs become non-operational, requiring repair of communication to restore functionality. The impact of such failures is quantified by linking affected devices to the repair time.

To identify these areas, we design an intelligent algorithm, i.e., Algorithm 1, that uses a traversal-based method to trace downstream nodes affected by link failures, following the network topology. It simulates how a control center sends confirmation signals to communication nodes. If no response is received from a node, that node is marked as affected and included in the cyber blind area. Algorithm 1 helps estimate the scope of communication failures and reasonably reflects how such issues are identified in practice.

$$\begin{cases} A^{\text{CR}}_i = Mz^{\text{comp}}_c + \max A^{\text{comp}}_{e(c)} \\ z^{\text{comp}}_c = numel(e(c)) - \sum_f \sum_{e(c)} \sum_{cmc} x_{f,e(c),cfrc} \end{cases}$$
$$\forall i \in N_c, \forall c \in C, \forall e(c) \in V^{\text{CN}}_{cfrc} \backslash DP, \forall f \in V^{\text{CN}}_{cfrc} \quad (19)$$

where $numel(e(c))$ calculates the number of communication failures $e(c)$ that cause the cyber blind area c in vertex e. In (19), we consider that a cyber blind area c may be caused by multiple communication failures $e(c)$. For a communication node i in a cyber blind area c, the communication function is restored only when all communication failures leading to the formation of c are repaired, i.e., $z^{\text{comp}}_c=0$. Thus, A^{CR}_i is equal to $\max A^{\text{comp}}_{e(c)}$, which represents the maximum repair completion time for upstream damaged communication failures on the same feeder. Otherwise, $z^{\text{comp}}_c>0$, so A^{CR}_i will be set to be a large value. Additionally, t^{CR}_i is set to be 0 if the communication node i is not in cyber blind areas.

Algorithm 1: searching all cyber blind areas and communication nodes contained

Input: topology of CPDS, V^{CN}_{cfrc}, NB_a

Output C, N_c

```
Establish an adjacency matrix based on topology of CPDS (representing a directed graph where the direction is from communication node to its command center)
Set a = 1, c = 1
for all e ∈ V^CN_cfrc \ DP do
  Obtain nodes and lines in block a
  if e ∈ NB_a then
    Obtain downstream node i of damaged communication line e
    for all j ∈ NB_a do
      Obtain communication upstream/downstream relationship and path scheme L set between i and j
      if P ≠ ∅ and i is downstream node of j then
        Place j into cyber blind area c
      end if
    end for
  end if
  a = a + 1, c = c + 1
end for
```

We assume that the RCS and VSC can only accept action commands when the communication functions of the nodes on both sides are intact. As outlined in Section II-A, the restoration time for the communication functions of the nodes on both sides of the RCS and VSC is dependent on ECVs and CFRCs. Binary variables u^{ECV}_a and u^{CFRC}_a indicate whether the communication function of the RCS and VSC is restored by ECV or CFRC.

$$u^{\text{ECV}}_a + u^{\text{CFRC}}_a \le 1 \quad \forall a \in \Omega_{\text{VSC}} \bigcup \Omega_{\text{RCS}} \quad (20)$$

If the communication function of the component at vertex a is repaired by ECV, i.e., $u^{\text{ECV}}_a=1$, the time at which the component at a can be controlled is set as $A^{\text{ECV}}_a=\sum_{ecv} A^{\text{leave}}_{b,ecv}$ by constraint (21). Accordingly, since the component at vertex a is not repaired by the CFRC, $u^{\text{CFRC}}_a=0$, and A^{CFRC}_a is set to be 0 by constraint (22).

If the communication function on both sides of the compo-

nent in block a is repaired by CFRC, i.e., $u_a^{\mathrm{CFRC}}=1$, the time is set as $A_a^{\mathrm{CFRC}}=\max(A_i^{\mathrm{CR}},A_j^{\mathrm{CR}})$ by constraint (22). That is the maximum value of the recovery time of the communication function of the nodes on both sides. Accordingly, since the component at vertex a is not repaired by the ECV, $u_a^{\mathrm{ECV}}=0$, and A_a^{ECV} is set to be 0 by constraint (21).

$$\begin{cases} 0\le A_a^{\mathrm{CR,ECV}}\le Mu_a^{\mathrm{ECV}} \\ A_a^{\mathrm{CR,ECV}}\ge \sum_{ecv} A_{a,ecv}^{\mathrm{reach}}+T_{a,ecv}^{\mathrm{stay}}-M(1-u_a^{\mathrm{ECV}}) \\ A_a^{\mathrm{CR,ECV}}\le \sum_{ecv} A_{a,ecv}^{\mathrm{reach}}+T_{a,ecv}^{\mathrm{stay}} \end{cases} \quad \forall a\in \Omega_{\mathrm{VSC}}\cup\Omega_{\mathrm{RCS}} \tag{21}$$

$$\begin{cases} 0\le A_a^{\mathrm{CR,CFRC}}\le Mu_a^{\mathrm{CFRC}} \\ A_a^{\mathrm{CR,CFRC}}\ge \max(A_i^{\mathrm{CR}},A_j^{\mathrm{CR}})-M(1-u_a^{\mathrm{CFRC}}) \\ A_a^{\mathrm{CR,CFRC}}\le \max(A_i^{\mathrm{CR}},A_j^{\mathrm{CR}}) \end{cases} \quad \forall a\in \Omega_{\mathrm{VSC}}\cup\Omega_{\mathrm{RCS}} \tag{22}$$

Finally, constraint (23) is utilized to determine the time when the component a can be successfully controlled.

$$\begin{cases} A_a^{\mathrm{CR}}\ge A_a^{\mathrm{CR,ECV}} \\ A_a^{\mathrm{CR}}\ge A_a^{\mathrm{CR,CFRC}} \end{cases} \quad \forall a\in \Omega_{\mathrm{VSC}}\cup\Omega_{\mathrm{RCS}} \tag{23}$$

D. System Recovery Model

Considering the coupling of the cyber and physical systems, we address the DSR problem by co-optimizing the scheduling of PFRCs, CFRCs, ECVs, and DGs, the RCS sequential action strategies, and the adaptive switching of VSC control modes to achieve a gradual restoration of the power supply after a disaster. The system recovery model can be divided into two parts: network reconfiguration constraints and distribution system operation constraints.

1) Network Reconfiguration Constraints

Existing research typically employs spanning tree theory to ensure radial configurations of AC distribution systems. For instance, a bus controlling voltage is designated as the root bus with no parent, while a non-voltage-controlling bus has at most one parent. A method that leverages the spanning tree theory is proposed for adaptive switching of VSC control modes, enhancing flexibility in network reconfiguration.

If line ij is connected during period t, the connection state $y_{ij,t}^{\mathrm{AC}}=1$; otherwise, $y_{ij,t}^{\mathrm{AC}}=0$. If bus i is the parent of bus j at period t, $f_{ij,t}^{\mathrm{AC}}=1$; otherwise, $f_{ij,t}^{\mathrm{AC}}=0$.

$$\begin{cases} f_{ij,t}^{\mathrm{AC}}+f_{ji,t}^{\mathrm{AC}}=s_{ij,t}^{\mathrm{AC}} & \forall ij\in B^{\mathrm{AC}},\forall t \\ f_{ij,t}^{\mathrm{DC}}+f_{ji,t}^{\mathrm{DC}}=s_{ij,t}^{\mathrm{DC}} & \forall ij\in B^{\mathrm{DC}},\forall t \end{cases} \tag{24}$$

$$\begin{cases} \sum_j f_{ji,t}^{\mathrm{AC}}=r_{i,t} & \forall i\in N^{\mathrm{AC}},\forall t \\ \sum_j f_{ji,t}^{\mathrm{DC}}=r_{i,t} & \forall i\in N^{\mathrm{DC}},\forall t \end{cases} \tag{25}$$

$$\begin{cases} r_{i,t}\le s_{i,t} & \forall i\in N_{\mathrm{VSC}}^{\mathrm{AC}}\cup N_{\mathrm{VSC}}^{\mathrm{DC}},\forall t \\ r_{i,t}=s_{i,t} & \forall i\in N\backslash N_{\mathrm{VSC}}^{\mathrm{AC}}\cup N_{\mathrm{VSC}}^{\mathrm{DC}},\forall t \\ r_{i,t}=0 & \forall i\in N_{\mathrm{sub}},\forall t \end{cases} \tag{26}$$

$$\begin{cases} f_{ik,t}^{\mathrm{AC}}=f_{kj,t}^{\mathrm{DC}} \\ f_{ki,t}^{\mathrm{AC}}=f_{jk,t}^{\mathrm{DC}} \\ y_{ik,t}^{\mathrm{AC}}=y_{kj,t}^{\mathrm{DC}} \end{cases} \quad \forall ij\in B_{\mathrm{VSC}},\forall t \tag{27}$$

Constraint (24) enforces that a unidirectional parent-child relationship between nodes at both ends of an AC/DC line exists only if the line is connected, ensuring unique tree-like topologies. Constraint (25) mandates that each energized regular AC/DC node (non-substation, non-VSC) must have exactly one parent node to maintain connectivity and prevent loops. Constraint (26) specifies root node rules: energized VSC nodes may serve as roots, regular AC/DC nodes cannot be roots regardless of energization status, and substation nodes are always roots. Constraint (27) ensures the operation consistency for interconnection lines of VSC by preventing simultaneous root assignment to both terminal nodes and synchronizing the connectivity states of paired AC/DC lines.

As established in Section II-A, the classification of faults to the AC side or DC side of the VSC has certain flexibility and must be combined with topology reconfiguration constraints. Consequently, constraint (28) integrates the topology reconfiguration constraints (24)-(27) with the voltage support requirement constraint (1). When the VSC switches to voltage control mode, the constraint is enforced. Upon switching to P-Q control mode, the constraint is relaxed. Crucially, the control mode of VSC is determined by the current outcome of topology reconfiguration. This interdependence establishes a topology-based adaptive switching model that dynamically selects the appropriate VSC control mode under the current system state.

$$U_{i,t}\ge U_0+r_{i,t}(U_i^{\min}-U_0)-M(1-s_{i,t}) \quad \forall i\in N_{\mathrm{VSC}}^{\mathrm{AC}}\cup N_{\mathrm{VSC}}^{\mathrm{DC}},\forall t \tag{28}$$

Specifically, constraint (28) specifies voltage constraints based on the energized and root status of bus, i.e., $s_{i,t}=1$, $r_{i,t}=0$. Then, its voltage constraint is $U_{i,t}\ge U_0$. If bus i is energized and is not the root node, i.e., $s_{i,t}=1$, $r_{i,t}=1$, $U_{i,t}\ge U_i^{\min}$; if bus i is not energized, i.e., $s_{i,t}=0$, $r_{i,t}=0$, the voltage is relaxed to $U_{i,t}\ge U_0-M$.

2) Distribution System Operation Constraints

The AC power flow constraints are based on the DistFlow model, with constraint (29) ensuring active and reactive power balance at each node, and constraint (30) limiting the voltage drop across the line. By simplifying the AC power flow constraints, the DC power flow constraints are established as (31) and (32).

$$\begin{cases} \sum_{j\in ds(i)} P_{i,j,t}-\sum_{j\in us(i)} P_{i,j,t}=P_{i,t}^{\mathrm{G}}-P_i^{\mathrm{load}}s_{i,t} \\ \sum_{j\in ds(i)} Q_{i,j,t}-\sum_{j\in us(i)} Q_{j,i,t}=Q_{i,t}^{\mathrm{G}}-Q_i^{\mathrm{load}}s_{i,t} \end{cases} \quad \forall i\in N^{\mathrm{AC}},\forall t \tag{29}$$

$$\begin{cases} U_{i,t}^2-U_{j,t}^2\le 2(R_{i,j}P_{i,j,t}+X_{i,j}Q_{i,j,t})+M(1-s_{ij,t}) \\ U_{i,t}^2-U_{j,t}^2\ge 2(R_{i,j}P_{i,j,t}+X_{i,j}Q_{i,j,t})-M(1-s_{ij,t}) \end{cases} \quad \forall ij\in B^{\mathrm{AC}},\forall t \tag{30}$$

$$\sum_{j\in ds(i)} P_{i,j,t}-\sum_{j\in us(i)} P_{j,i,t}=P_{i,t}^{\mathrm{G}}-P_i^{\mathrm{load}}s_{i,t} \quad \forall i\in N^{\mathrm{DC}},\forall t \tag{31}$$

$$\begin{cases} U_{i,t}^2 - U_{j,t}^2 \le 2R_{i,j}P_{i,j,t} + M(1-s_{ij,t}) \\ U_{i,t}^2 - U_{j,t}^2 \ge 2R_{i,j}P_{i,j,t} - M(1-s_{ij,t}) \end{cases} \quad \forall ij \in B^{\mathrm{DC}}, \forall t \tag{32}$$

Additional security constraints include limits on line power (33), node generation capacity (34), and node voltage (35), while ensuring that all loads are restored (36). Among them, (35) ensures that the voltages of all nodes remain within a safe range during the switching process of VSC control modes.

$$\begin{cases} -P_{i,j}^{\max} s_{i,j,t} \le P_{i,j,t} \le P_{i,j}^{\max} s_{ij,t} \\ -Q_{i,j}^{\max} s_{i,j,t} \le Q_{i,j,t} \le Q_{i,j}^{\max} s_{ij,t} \end{cases} \quad \forall ij \in B, \forall t \tag{33}$$

$$\begin{cases} 0 \le P_{i,t}^{\mathrm{G}} \le P_i^{\max} s_{i,t} \\ 0 \le Q_{i,t}^{\mathrm{G}} \le Q_i^{\max} s_{i,t} \end{cases} \quad \forall i \in N_{\mathrm{G}}, \forall t \tag{34}$$

$$U_i^{\min} s_{i,t} \le U_{i,t} \le U_i^{\max} s_{i,t} \quad \forall i \in N, \forall t \tag{35}$$

$$\sum_t s_{i,t} \ge 1 \quad \forall i \in N \tag{36}$$

E. Constraints of Coupling Relations

The units of time in the scheduling model of multi-type repair resources and the system recovery model are fundamentally inconsistent, so they cannot be directly coordinated. Specifically, in the system recovery model, system scheduling operates in discrete intervals of 30 min. Meanwhile, in the adaptive switching model, component repair time and path traversal time are modeled as continuous values in minutes, and may not align with the 30 min scheduling boundaries. Therefore, it is necessary to map the exact moment of completing the maintenance of system component to its corresponding discrete time interval.

$$\begin{cases} \sum_{t=1}^{T^{\mathrm{p}}} (t-1)\alpha_{m,t}^{\mathrm{ER}} \Delta t \ge \sum_{pfrc} A_{m,pfrc}^{\mathrm{leave}} \\ \sum_{t=1}^{T^{\mathrm{p}}} (t-1)\alpha_{m,t}^{\mathrm{ER}} \Delta t < \sum_{pfrc} A_{m,pfrc}^{\mathrm{leave}} + \Delta t \\ \sum_{t=1}^{T^{\mathrm{p}}} \alpha_{m,t}^{\mathrm{ER}} = 1 \end{cases} \quad \forall m \in V_{pfrc}^{\mathrm{EN}}, \forall t \tag{37}$$

$$\sum_1^{\tau} \alpha_{m,t}^{\mathrm{ER}} = \beta_{m,\tau}^{\mathrm{ER}} \quad \forall m \in V_{pfrc}^{\mathrm{EN}}, \forall \tau \tag{38}$$

$$\begin{cases} \sum_{t=1}^{T^{\mathrm{p}}} (t-1)\alpha_{a,t}^{\mathrm{CR}} \Delta t \ge A_a^{\mathrm{CR}} \\ \sum_{t=1}^{T^{\mathrm{p}}} (t-1)\alpha_{a,t}^{\mathrm{CR}} \Delta t < A_a^{\mathrm{CR}} + \Delta t \end{cases} \quad \forall a \in \Omega_{\mathrm{VSC}} \bigcup \Omega_{\mathrm{RCS}} \tag{39}$$

$$\sum_{t=1}^{\tau} \alpha_{a,t}^{\mathrm{CR}} = \beta_{a,\tau}^{\mathrm{CR}} \quad \forall a \in \Omega_{\mathrm{VSC}} \bigcup \Omega_{\mathrm{RCS}}, \forall \tau \tag{40}$$

Constraint (37) maps the time of completing maintenance $A_{m,pfrc}^{\mathrm{leave}}$ of power component m to the discrete time interval t of the DSR optimization decision. Specifically, $\alpha_{m,t}^{\mathrm{ER}}$ indicates whether the electrical function of component m has been restored to normal during time period t, which is based on the time of completing its maintenance work $\sum_{pfrc} A_{m,pfrc}^{\mathrm{leave}}$. If so, $\alpha_{m,t}^{\mathrm{ER}} = 1$; otherwise, $\alpha_{m,t}^{\mathrm{ER}} = 0$. Constraint (38) determines whether the functionality of m is intact in each time interval τ. Specifically, $\beta_{m,\tau}^{\mathrm{ER}}$ determines whether component m is electrically functional during time period τ based on $\alpha_{m,t}^{\mathrm{ER}}$. If yes, $\beta_{m,\tau}^{\mathrm{ER}} = 1$; otherwise, $\beta_{m,\tau}^{\mathrm{ER}} = 0$.

Similarly, constraint (39) maps the time of completing maintenance A_a^{CR} of communication component a to the discrete time interval t of the DSR optimization decision. If A_a^{CR} belongs to period t, $\alpha_{a,t}^{\mathrm{CR}} = 1$; otherwise, $\alpha_{a,t}^{\mathrm{CR}} = 0$. Constraint (40) determines whether the functionality of a is intact in each time interval τ. If yes, $\beta_{a,\tau}^{\mathrm{CR}} = 1$; otherwise, $\beta_{a,\tau}^{\mathrm{CR}} = 0$.

Next, the power fault state and communication fault state must be linked to the on/off status of the line. In practice, not all lines are equipped with RCSs due to cost constraints. However, it is sufficient to control critical lines with RCSs to enhance the overall flexibility. In this paper, certain critical lines are selected to be configured with RCSs.

For these lines equipped with RCSs and VSCs, the master station can only successfully send signals to complete switching actions of VSC control mode when both electric and communication functions are intact. This relationships are expressed as (41) amd (42) when the fault m happens on line ij and when component a is on line ij, respectively:

$$\beta_{m,t}^{\mathrm{ER}} \ge s_{ij,t} \quad \forall m \in V_{erc}^{\mathrm{EN}} \tag{41}$$

$$\beta_{a,t}^{\mathrm{CR}} \ge s_{ij,t} \quad \forall a \in \Omega_{\mathrm{VSC}} \bigcup \Omega_{\mathrm{RCS}} \tag{42}$$

F. Proposed Optimization Framework

The objective of the propsed optimization framework is to restore the power supply of all loads and minimize the load curtailment during the recovery process. The objective function is formulated as:

$$\min \sum_{i \in N} \sum_t \omega_i (1 - s_{i,t}) P_i^{\mathrm{load}} \tag{43}$$

The proposed optimization framework contains the following constraints: ① adaptive switching of VSC control modes and power control (2) - (5), (28); ② dispatching constraints for PFRCs, CFRCs, and ECVs (6) - (18); ③ impact of communication failures (19) - (23); ④ radial energization path constraints (24) - (27); ⑤ operation and safety constraints (29)-(36); ⑥ constraints of coupling relations (37)-(42).

III. Solution Method

The proposed optimization framework is a mixed-integer non-convex formulation, which is difficult to solve in practice, especially for large-scale post-disaster recovery. Commercial solvers such as CPLEX or Gurobi often struggle to find feasible solutions in a reasonable time. This is mainly because many binary variables and non-convex power flow constraints are included, leading to a rapid increase in computational complexity [18].

To solve the problem efficiently, we adopt three methods: ① the fault pre-assignment method is applied to reduce computational burden; ② the linearization method is applied for nonlinear constraints; ③ conic relaxation method is applied to convert the non-convex problem into a mixed-integer second-order cone programming (MISOCP) problem.

A. Fault Pre-assignment Method

In the proposed model, PFRCs and CFRCs may be dispatched to each fault, leading to a large number of binary variables and increased computational complexity. To reduce this burden, we apply the fault pre-assignment method based on the proximity principle, assigning repair tasks to each depot. Thus, PFRC at depot *dp* is only dispatched to a fault pre-assigned to *dp*.

The fault pre-assignment method of power fault is expressed as:

$$\min \sum_{p}\sum_{m} l_{dp,m} u_{dp,m}^{\mathrm{FPM}} \tag{44}$$

$$\sum_{dp} u_{dp,m}^{\mathrm{FPM}} = 1 \quad \forall m \in V_{cfrc}^{\mathrm{EN}} \backslash D \tag{45}$$

The objective function (44) indicates that the repair tasks of power faults are pre-assigned to each station according to the proximity principle. Constraint (45) ensures that each damaged electric line is assigned to a depot.

In the original model formulation, constraints related to routing problems and scheduling problem result in a computational complexity of $O(M^3)$. Specifically, for N_{D} depots and M faults, the routing requires considering all possible fault-to-fault paths, leading to complexity of $O(M^2 N_{\mathrm{D}})$. When the number of faults M is similar to those of resources K and time windows T, the three-dimensional constraints of dynamic scheduling increase the computational complexity to $O(M^3)$. With the fault pre-assignment method (assuming that faults are evenly distributed), the routing complexity is reduced to $O(D(M/N_{\mathrm{D}})^2)=O(M^2/N_{\mathrm{D}})$, and the scheduling complexity becomes $O(D(M/N_{\mathrm{D}})^3)=O(M^3/N_{\mathrm{D}}^2)$. This method reduces the number of variables and constraints and lowers the overall complexity by two orders of magnitude, thereby improving computational efficiency without compromising the solution quality.

B. Linearization Method

Reference [28] reveals that the nonlinear branch loss term is much smaller than the branch power term in practice. Therefore, based on the idea of the LinDistFlow model in [29], to accelerate the solution, we eliminate the quadratic terms for the power loss in VSC and branches in (2), (4), (5), (30), and (32). Moreover, variable substitution is utilized to linearize the quadratic terms, i.e., substituting $U_{i,t}^2$ with $U_{i,t}^{\mathrm{sqr}}$, thus converting the nonlinear constraints into linear ones.

$$\begin{cases} P_{i,ka,t} = P_{k,t} = P_{kd,j,t} \\ Q_{i,ka,t} = -Q_{k,t} \end{cases} \quad \forall k \in \Omega_{\mathrm{VSC}}, \forall t \tag{46}$$

$$\begin{cases} U_{i,t}^{\mathrm{sqr}} - U_{ka,t}^{\mathrm{sqr}} \le 2(R_{i,ka}P_{i,ka,t} + X_{i,ka}Q_{i,ka,t}) + M(1-s_{i,ka,t}) \\ U_{i,t}^{\mathrm{sqr}} - U_{ka,t}^{\mathrm{sqr}} \ge 2(R_{i,ka}P_{i,ka,t} + X_{i,ka}Q_{i,ka,t}) - M(1-s_{i,ka,t}) \end{cases} \quad \forall k \in \Omega_{\mathrm{VSC}}, k \text{ is on line } ij, \forall t \tag{47}$$

$$\begin{cases} U_{kd,t}^{\mathrm{sqr}} - U_{j,t}^{\mathrm{sqr}} \le 2R_{kd,j}P_{kd,t} + M(1-s_{kd,j,t}) \\ U_{kd,t}^{\mathrm{sqr}} - U_{j,t}^{\mathrm{sqr}} \ge 2R_{kd,j}P_{kd,t} - M(1-s_{kd,j,t}) \end{cases} \quad \forall k \in \Omega_{\mathrm{VSC}}, k \text{ is on line } ij, \forall t \tag{48}$$

$$\begin{cases} U_{i,t}^{\mathrm{sqr}} - U_{j,t}^{\mathrm{sqr}} \le 2(R_{i,j}P_{i,j,t} + X_{i,j}Q_{i,j,t}) + M(1-s_{ij,t}) \\ U_{i,t}^{\mathrm{sqr}} - U_{j,t}^{\mathrm{sqr}} \ge 2(R_{i,j}P_{i,j,t} + X_{i,j}Q_{i,j,t}) - M(1-s_{ij,t}) \end{cases} \quad \forall ij \in B^{\mathrm{AC}}, \forall t \tag{49}$$

$$\begin{cases} U_{i,t}^{\mathrm{sqr}} - U_{j,t}^{\mathrm{sqr}} \le 2R_{i,j}P_{i,j,t} + M(1-s_{ij,t}) \\ U_{i,t}^{\mathrm{sqr}} - U_{j,t}^{\mathrm{sqr}} \ge 2R_{i,j}P_{i,j,t} - M(1-s_{ij,t}) \end{cases} \quad \forall ij \in B^{\mathrm{DC}}, \forall t \tag{50}$$

C. Conic Relaxation

By using convic relaxation, (3) can be converted to rotated quadratic cone constraints, which are given as:

$$\begin{cases} -S_k^{\mathrm{VSC}} s_{ij,t} \le P_{k,t}^{\mathrm{VSC}} \le S_k^{\mathrm{VSC}} s_{ij,t} \\ -S_k^{\mathrm{VSC}} s_{ij,t} \le Q_{k,t}^{\mathrm{VSC}} \le S_k^{\mathrm{VSC}} s_{ij,t} \\ -\sqrt{2}\, S_k^{\mathrm{VSC}} s_{ij,t} \le P_{k,t}^{\mathrm{VSC}} + Q_{k,t}^{\mathrm{VSC}} \le \sqrt{2}\, S_k^{\mathrm{VSC}} s_{ij,t} \\ -\sqrt{2}\, S_k^{\mathrm{VSC}} s_{ij,t} \le P_{k,t}^{\mathrm{VSC}} - Q_{k,t}^{\mathrm{VSC}} \le \sqrt{2}\, S_k^{\mathrm{VSC}} s_{ij,t} \\ Q_k^{\min} s_{ij,t} \le Q_{k,t}^{\mathrm{VSC}} \le Q_k^{\max} s_{ij,t} \end{cases} \quad \forall k \in \Omega_{\mathrm{VSC}}, k \text{ is on line } ij, \forall t \tag{51}$$

D. Tractable Optimization Framework

The second-order conic relaxation is used to relax certain non-convex constraints, enabling faster computation while maintaining acceptable solution accuracy [30]. In parallel, equivalent linearization method is applied to address other nonlinear components [31].

As a result, the reformulated MISOCP problem achieves a balanced trade-off between computational efficiency and solution quality, consistent with findings from previous studies. Therefore, the obtained results closely match those of the original problem within an acceptable range [30] and can be efficiently solved by the optimization solver Gurobi [10], [31]. Finally, to achieve the collaborative and efficient recovery, the complete form of the proposed optimization framework can be expressed in detail as:

$$\min \sum_{i \in N}\sum_{t} \omega_i (1 - s_{i,t}) P_i^{\mathrm{load}} \tag{52}$$

s.t.

1) VSC constraints (2), (28), (51), (46), and (47).
2) Scheduling of multi-type repair resources (6)-(18).
3) Impact of communication failures (19)-(23).
4) Reconfiguration (24)-(27).
5) Power flow (29), (31), (33)-(36), (49), and (50).
6) Coupling relations (37)-(42).

IV. Case Study

The proposed optimization framework is applied in a modified IEEE 123-bus test system, in which a portion of AC grid is modified to a DC grid. The system operates at 4.16 kV with a total load demand of 4330 kW. The CPDSs include a command center, three depots, four VSCs, eight RCSs, six DGs, and two substations. Before the disaster occurs, VSCs adopt a master-slave control: VSC4, which is directly interfaced with a stable external power source and possesses relatively larger capacity, is designated as the master VSC

operating in V_{DC}-Q control mode to regulate the DC network voltage, while VSC1, VSC2, and VSC3 function as slave converters operating in P-Q control mode. A converter station with relatively large capacity is typically selected as the master station, tasked with maintaining the DC bus voltage. In this paper, VSC4 is directly connected to an external power source, providing stable and reliable power. Hence, it is appropriately configured as the master VSC, responsible for regulating the DC voltage across the network. We assume that 12 power lines and 10 communication links are damaged, as shown in Fig. 4.

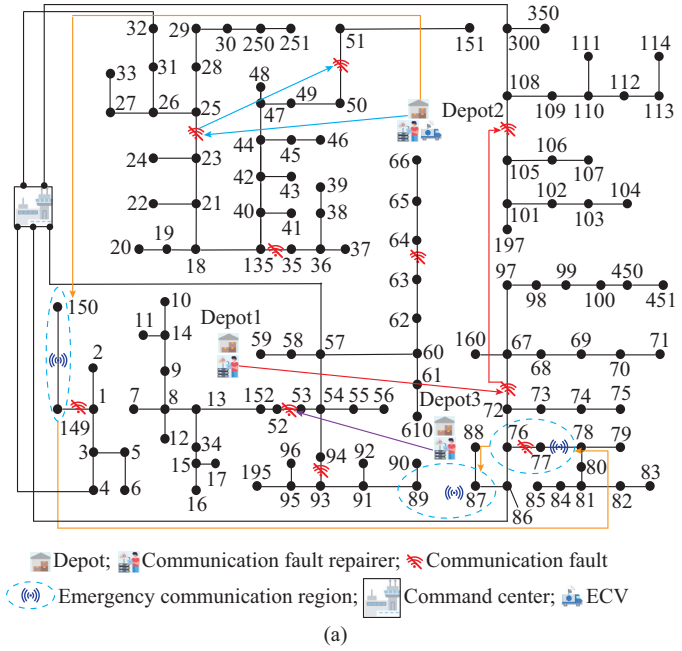

Fig. 4. Modified IEEE 123-bus test system. (a) Communication fault. (b) Electric fault.

Each depot is equipped with two EFRCs and a CFRC, while depot 2 additionally includes an ECV. The repair time, operation time of RCS, and switching time of VSC control modes are considered, with specific values available in Supplementary Material A Tables SAI-SAIII. Note that different colors of arrows in Fig. 4 represent different repair groups.

All simulations are conducted in MATLAB R2023a with Gurobi 10.0.3 on a desktop (Intel Core i7-13700, 32 GB RAM, 64-bit OS).

A. Analysis of Effectiveness of Proposed Optimization Framework

The proposed optimization framework is solved in 809.78 s. All the loads are restored within 330 min, and the total restored energy reaches 19893.50 kWh. The dispatching path result of PFRCs is shown in Supplementary Material A Fig. SA1, while the dispatching path results of CFRCs and ECV are shown in Supplementary Material A Fig. SA2. Their travel paths and timetables are given in Table I.

TABLE I
TRAVEL PATHS AND TIMETABLES FOR THREE TYPES OF REPAIR RESOURCES

Depot	Crew	Travel path (arriving/leaving time (min))
1	PFRC1	18-19 (22/113)→25-26 (143/250)
	PFRC2	7-8 (25/78)→13-34 (116/191)→1-3 (221/319)
2	PFRC3	109-110 (32/143)→101-105 (188/308)
	PFRC4	44-47 (17/93)→35-36 (109/221)
3	PFRC5	67-160 (42/84)
	PFRC6	76-86 (23/66)→89-91 (90/141)
1	CFRC1	67-72 (27/64)→105-108 (97/155)
2	CFRC2	23-25 (31/70)→50-51 (89/139)
	ECV	149-150 (57/90)→76-77 (109/120)→87-89 (150/180)
3	CFRC3	52-53 (21/73)

To detail the sequential recovery process of the CPDSs, the restoration schedule is outlined in Supplementary Material A Table SAIV. The collaborative recovery tasks include: ① repairing damaged power lines and communication links; ② restoring communication functionality of RCSs and VSCs; ③ sequencing RCS switching actions; ④ sequencing VSC control mode adjustments; and ⑤ determining the energization sequence of each node and DG with power generation.

The adaptive switching is the key to ensuring the co-optimization of the VSC control modes, the scheduling of repair resources, and the restoration of the power supply. Supplementary Material A Table SAV demonstrates the control modes and related parameters of the VSC at several critical time instants.

In the proposed optimization framework, the system is allowed to operate in a multi-island configuration during recovery to maximize load restoration. However, the system does not operate in this mode under normal conditions. Although all faults are repaired within 330 min, the system remains islanded (e. g., VSC3 is still in V_{AC}-f control mode) due to the flexibility permitted during restoration. This reflects the goal of DSR to restore power as quickly as possible, and therefore, does not include the process of restoring to the initial configuration prior to the disaster. The transition to initial configuration depends on subsequent schedul-

ing of utilities, which is beyond the scope of this paper and therefore not simulated.

B. Analysis of Superiority of Proposed Optimization Framework

To show the superiority of the proposed optimization framework, we design four cases and conduct a comprehensive comparison with existing methods in DSR. The cooperation of CFRCs and ECVs can accelerate the restoration of cyber system and improve the efficiency of DSR, which is a prominent feature of the developed models. Thus, three state-of-the-art models for restoring the CPDS with CFRCs or ECVs and an advanced hierarchical optimization model are built for comparison with the proposed optimization framework.

1) Case 1: based on hierarchical optimization [18], PFRC is first scheduled to minimize the repair time, and then the system restoration sequence is obtained by minimizing the load shedding according to the repair sequence (ignoring communication failures). The priority of communication failures is determined based on the importance of RCS/VSC communication functions in the restoration sequence, and CFRC repair is then scheduled according to this priority. Finally, the PFRC and CFRC scheduling results are fed into DSR to obtain the final restoration sequence.

2) Case 2: the PFRC/CFRC scheduling, system restoration, and adaptive switching of VSC control modes are optimized synchronously. This case demonstrates the advantages of synchronous optimization over hierarchical optimization (Case 1) under the constraint that PFRC and CFRC work independently [21].

3) Case 3: coordinated repair by CFRC and ECV is introduced, enhancing the communication restoration capability. However, it maintains the fixed VSC control mode throughout restoration [7]. This case highlights the advantages of flexibly exploiting communication resources to coordinate work.

4) Case 4: the proposed optimization framework coordinates the dispatch of PFRCs, CFRCs, ECV, and the adaptive switching of VSC control modes to accelerate the load restoration of the CPDSs depicted in previous sections.

The settings of the four cases are summarized in Table II.

TABLE II
SETTINGS OF FOUR CASES

Case	Repair mode	VSC control model	Dispatchable resources	Optimization structure
1	Independent [21] (separate)	Adaptive switching	6 PFRCs, 4 CFRCs	Hierarchical [18]
2	Independent [21] (simultaneous)	Adaptive switching	6 PFRCs, 4 CFRCs	Synchronous
3	Coordinated (CFRC + ECV)	Fixed [7]	6 PFRCs, 3 CFRCs, 1 ECV	Synchronous
4	Coordinated (CFRC + ECV)	Adaptive switching	6 PFRCs, 3 CFRCs, 1 ECV	Synchronous

A comprehensive comparison of total restored power and energy of loads in the four cases is illustrated in Fig. 5 and Fig. 6, respectively, and the analysis of the results is described as follows. Detailed recovery timelines, quantitative energy comparisons, and voltage deviation statistics are provided in Supplementary Material A.

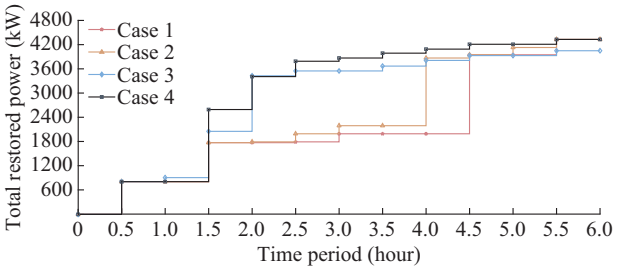

Fig. 5. Comparison of total restored power of loads in four cases.

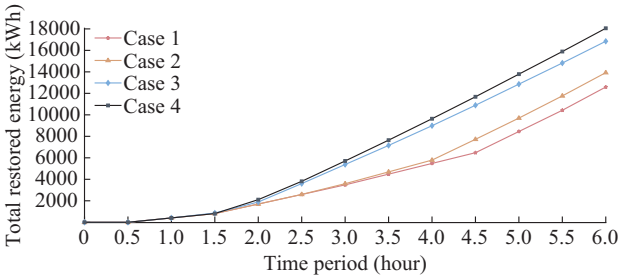

Fig. 6. Comparison of total restored energy of loads in four cases.

When PFRC, CFRC, and ECV are scheduled independently (Case 1), the lack of coordination leads to asynchronous recovery between cyber and physical systems, causing extended delays in load restoration. With synchronous scheduling (Case 2), these idle gaps are eliminated and the efficiency of system recovery is remarkably improved.

The comparison between Cases 2 and 4 demonstrates the importance of coordinating different types of communication restoration resources. CFRCs are more effective when the communication repair can be completed quickly, while ECVs provide immediate wireless connectivity when power repair is completed earlier. By jointly optimizing both resources, Case 4 achieves consistently higher recovery levels and total restored energy, confirming the superiority of cooperation.

The comparison between Cases 3 and 4 demonstrates two key advantages of adaptive switching of VSC control modes. First, by dynamically adjusting control modes during the recovery process, Case 4 achieves higher restoration efficiency than the fixed mode of Case 3, which is constrained by its inability to adapt to evolving system conditions. Second, as illustrated in Fig. 7, the adaptive switching model significantly reduces both the average and maximum voltage deviations, fully leveraging the voltage control capability of VSC to provide stable support for energized nodes. Together, these results confirm that the adaptive switching model enhances both recovery efficiency and voltage stability. On average, the co-optimization in Cases 2-4 achieves 29.3% higher total recovered energy than the hierarchical optimization in Case 1, demonstrating its superior performance. Additionally, incorporating ECVs as a key repair resource for restoring communication functions significantly enhances the efficiency of load recovery. On average, the amount of total recovered energy in Cases 3 and 4 is 31.6% higher than that in Cases 1 and 2, where only CFRCs are involved in communication restoration.

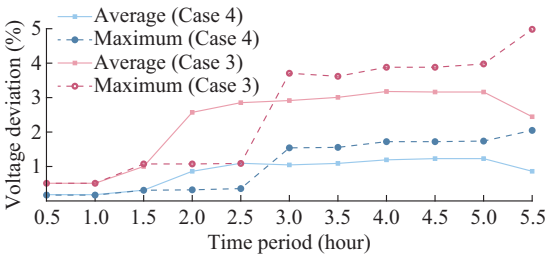

Fig. 7. Average and maximum voltage deviation for each period.

V. Conclusion

This paper proposes a novel optimization framework for HDSs to accelerate the post-disaster service restoration. By coordinating VSC control modes and repair resources across cyber and physical systems, the proposed optimization framework significantly improves recovery speed and energy efficiency, as validated on a modified IEEE 123-bus system.

Based on the results in this paper, several future research directions emerge to address operation challenges under extreme events.

1) Disaster path simulation can be integrated into the optimization process by using probabilistic hazard trajectory models. This supports proactive fault prediction and more efficient crew deployment, helping to reduce delays and avoid misallocation of resources.

2) Dynamic safety constraints for AC/DC hybrid systems merit attention. Existing restoration methods often treat voltage and frequency as static parameters, which may not hold in times of fast transients. Utilizing simplified transient stability models can introduce safety margins for frequency-voltage limits, ensuring the stability of newly formed islands during energization.

3) Uncertainties in DSR data such as travelling time of repair crews and the intermittency of renewable energy can greatly affect the scheduling outcomes and system recovery, and should be further explored through uncertainty-aware modeling.

References

[1] L. Zhang, B. Tong, Z. Wang *et al.*, "Optimal configuration of hybrid AC/DC distribution network considering the temporal power flow complementarity on lines," *IEEE Transactions on Smart Grid*, vol. 13, no. 5, pp. 3857-3866, Sept. 2022.

[2] Z. Yang, H. Wang, W. Liao *et al.*, "Protection challenges and solutions for AC Systems with renewable energy sources: a review," *Protection and Control of Modern Power Systems*, vol. 10, no. 1, pp. 18-39, Jan. 2025.

[3] J. Lu, C. Qin, Y. Zen *et al.*, "Collaborative recovery method for cyber-physical distribution system considering multiple coupling constraints," *Journal of Modern Power Systems and Clean Energy*, vol. 13, no. 5, pp. 1752-1762, Sept. 2025.

[4] L. Xu, Q. Guo, Y. Sheng *et al.*, "On the resilience of modern power systems: a comprehensive review from the cyber-physical perspective," *Renewable and Sustainable Energy Reviews*, vol. 152, p. 111642, Dec. 2021.

[5] X. Pan, L. Zhang, J. Xiao *et al.*, "Design and implementation of a communication network and operating system for an adaptive integrated hybrid AC/DC microgrid module," *CSEE Journal of Power and Energy Systems*, vol. 4, no. 1, pp. 19-28, Mar. 2018.

[6] L. Sun, H. Wang, Z. Huang *et al.*, "Coordinated islanding partition and scheduling strategy for service restoration of active distribution networks considering minimum sustainable duration," *IEEE Transactions on Smart Grid*, vol. 15, no. 6, pp. 5539-5554, Nov. 2024.

[7] Z. Chen, Z. Hu, Y. Wan *et al.*, "An extreme weather risk-averse planning method for soft open points considering distribution network reconfiguration," *Journal of Modern Power Systems and Clean Energy*, doi: 10.35833/MPCE.2025.000131

[8] P. Li, J. Ji, H. Ji *et al.*, "Self-healing oriented supply restoration method based on the coordination of multiple SOPs in active distribution networks," *Energy*, vol. 195, Mar. 2020.

[9] L. Zhang, C. Wang, J. Liang *et al.*, "A coordinated restoration method of hybrid AC/DC distribution network for resilience enhancement," *IEEE Transactions on Smart Grid*, vol. 14, no. 1, pp. 112-125, Jan. 2023,

[10] L. Zhang, S. Yu, B. Zhang *et al.*, "Outage management of hybrid AC/DC distribution systems: co-optimize service restoration with repair crew and mobile energy storage system dispatch," *Applied Energy*, vol. 335, p. 120422, Apr. 2023.

[11] J. Renedo, A. García-Cerrada, L. Rouco *et al.*, "Coordinated control in VSC-HVDC multi-terminal systems to improve transient stability: the impact of communication latency," *Energies*, vol. 12, no. 19, p. 19, Jan. 2019.

[12] Y. Ye, S. Liu, Z. Zhao *et al.*, "Cyber-physical co-optimization and control methods in smart grid," *Protection and Control of Modern Power Systems*, vol. 9, no. 4, pp. 1-2, Jul. 2024.

[13] W. Wang, Y. Li, Y. Cao *et al.*, "Adaptive droop control of VSC-MTDC system for frequency support and power sharing," *IEEE Transactions on Power Systems*, vol. 33, no. 2, pp. 1264-1274, Mar. 2018.

[14] H. Hou, J. Tang, Z. Zhang *et al.*, "Resilience enhancement of distribution network under typhoon disaster based on two-stage stochastic programming," *Applied Energy*, vol. 338, p. 120892, May 2023.

[15] Z. Ye, C. Chen, B. Chen *et al.*, "Resilient service restoration for unbalanced distribution systems with distributed energy resources by leveraging mobile generators," *IEEE Transactions on Industrial Informatics*, vol. 17, no. 2, pp. 1386-1396, Feb. 2021.

[16] X. Jiang, J. Chen, Q. Wu *et al.*, "Two-step optimal allocation of stationary and mobile energy storage systems in resilient distribution networks," *Journal of Modern Power Systems and Clean Energy*, vol. 9, no. 4, pp. 788-799, Jul. 2021.

[17] A. Arif, Z. Wang, C. Chen *et al.*, "Repair and resource scheduling in unbalanced distribution systems using neighborhood search," *IEEE Transactions on Smart Grid*, vol. 11, no. 1, pp. 673-685, Jan. 2020.

[18] G. Zhang, F. Zhang, X. Zhang *et al.*, "Sequential disaster recovery model for distribution systems with co-optimization of maintenance and restoration crew dispatch," *IEEE Transactions on Smart Grid*, vol. 11, no. 6, pp. 4700-4713, Nov. 2020.

[19] W. Sheng, K. Liu, Z. Li *et al.*, "Collaborative fault recovery and network reconstruction method for cyber-physical-systems based on double layer optimization," *CSEE Journal of Power and Energy Systems*, vol. 9, no. 1, pp. 380-392, Jan. 2023.

[20] X. Sun, J. Chen, H. Zhao *et al.*, "Sequential disaster recovery strategy for resilient distribution network based on cyber-physical collaborative optimization," *IEEE Transactions on Smart Grid*, vol. 14, no. 2, pp. 1173-1187, Mar. 2023.

[21] M. Tian, Z. Dong, L. Gong *et al.*, "Coordinated repair crew dispatch problem for cyber-physical distribution system," *IEEE Transactions on Smart Grid*, vol. 14, no. 3, pp. 2288-2300, May 2023.

[22] Z. Ye, C. Chen, R. Liu *et al.*, "Boost distribution system restoration with emergency communication vehicles considering cyber-physical interdependence," *IEEE Transactions on Smart Grid*, vol. 14, no. 2, pp. 1262-1275, Mar. 2023.

[23] H. Pan, H. Lian, C. Na *et al.*, "Modeling and vulnerability analysis of cyber-physical power systems based on community theory," *IEEE Systems Journal*, vol. 14, no. 3, pp. 3938-3948, Sept. 2020.

[24] Y. Wang, J. He, Y. Zhao *et al.*, "Equal loading rate based master-slave voltage control for VSC based DC distribution systems," *IEEE Transactions on Power Delivery*, vol. 35, no. 5, pp. 2252-2259, Oct. 2020.

[25] H. Alrajhi, A. Daraz, A. Alzahrani *et al.*, "Power sharing control trends, challenges, and solutions in multi-terminal HVDC systems: a comprehensive survey," *IEEE Access*, vol. 12, pp. 69112-69129, 2024.

[26] M. Ayiad, E. Maggioli, H. Leite *et al.*, "Communication requirements for a hybrid VSC based HVDC/AC transmission networks state estimation," *Energies*, vol. 14, no. 4, Art. no. 4, Jan. 2021.

[27] Y. Xiong, W. Yao, S. Lin *et al.*, "Improved communication-free coordinated control of VSC-MTDC integrated offshore wind farms for onshore system frequency support," *IEEE Transactions on Power Delivery*, vol. 40, no. 2, pp. 667-680, Apr. 2025.

[28] S. Lei, C. Chen, Y. Li *et al.*, "Resilient disaster recovery logistics of distribution systems: co-optimize service restoration with repair crew and mobile power source dispatch," *IEEE Transactions on Smart*

Grid, vol. 10, no. 6, pp. 6187-6202, Nov. 2019.
[29] M. E. Baran and F. Wu, "Optimal capacitor placement on radial distribution systems," *IEEE Transactions on Power Delivery*, vol. 4, no. 1, pp. 725-734, Jan. 1989.
[30] M. Farivar and S. H. Low, "Branch flow model: relaxations and convexification – Part I," *IEEE Transactions on Power Systems*, vol. 28, no. 3, pp. 2554-2564, Aug. 2013.
[31] X. Yang, C. Xu, J. Wen *et al.*, "Cooperative repair scheduling and service restoration for distribution systems with soft open points," *IEEE Transactions on Smart Grid*, vol. 14, no. 3, pp. 1827-1842, May 2023.

Xuyuan Gong received the B.S. degree from the School of Electrical Engineering, Chongqing University, Chongqing, China, in 2023. He is currently working toward the M.S. degree with the School of Electrical Engineering, Chongqing University. His current research interests include distribution system restoration, and operation optimization in power system.

Kaigui Xie received the Ph.D. degree in power system and its automation from Chongqing University, Chongqing, China, in 2001. He is a currently a Full Professor with the School of Electrical Engineering, Chongqing University. His research interests include power system reliability, planning, and analysis.

Changzheng Shao received the B.S. degree in electrical engineering from Shandong University, Jinan, China, and the Ph.D. degree in electrical engineering from Zhejiang University, Hangzhou, China, in 2015 and 2020, respectively. He is currently an Assistant Professor with Chongqing University, Chongqing, China. His research interests include operation optimization and reliability evaluation of integrated energy system.

Yifan Su received the B. Sc. and Ph. D. degrees in electrical engineering from Tsinghua University, Beijing, China, in 2019 and 2024, respectively. He is currently an Assistant Professor with Chongqing University, Chongqing, China. His research interests include distributed optimization and robust dispatch in smart grid.

Bo Hu received the Ph.D. degree in electrical engineering from Chongqing University, Chongqing, China, in 2010. He is currently a Full Professor with the School of Electrical Engineering, Chongqing University. His research interests include power system reliability and parallel computing techniques in power system.

Dong Zheng received the B.S. degree from Fuzhou University, Fuzhou, China, in 2021. He is currently working toward the Ph.D. degree with the State Key Laboratory of Power Transmission Equipment Technology, School of Electrical Engineering, Chongqing University, Chongqing, China. His research interests include reliability evaluation and dispatch of power system.